Rocznik Ochrona Środowiska

Volume 26 Year 2024 ISSN 2720-7501 pp. 356-365

https://doi.org/10.54740/ros.2024.034 open access

Received: June 2024 Accepted: August 2024 Published: August 2024

Three-dimensional-electrode Electrochemical Oxidation of Refractory Organic Matter in a Cold High-altitude Area: A Case Study of Dibutyl Phthalate

Xiaoyan Wei[1,2], Kang Li[1,2], Wanqi Wang[2,3], Tianhong Zhou[1], Jianjun Gao[4], Mingxia Jing[2], Aoxiang Cao[2], Kun Lu[2], Guozhen Zhang[1], Hao Wang[5**]*

[1]*School of Environmental and Municipal Engineering, Lanzhou Jiaotong University, China*

[2]*College of Civil Engineering and Hydraulic Engineering, Qinghai University, China*

[3]*School of Civil Engineering, Tianjin University, China*

[4]*Economic and Technological Development Bureau, Biotechnology Industrial Park Administrative Committee of Qinghai Province, China*

[5]*State Key Laboratory of Watershed Water Cycle Simulation and Regulation, China Institute of Water Resources and Hydropower Research, China*

[*]*corresponding author's e-mail: zhangguozhen@mail.lzjtu.cn*

[**]*corresponding author's e-mail: wanghao@iwhr.com*

Abstract: Qinghai has a high altitude, low average temperature and low oxygen concentration, but it has abundant power resources, so it has a good application prospect to use electrochemical oxidation to degrade refractory organic matter. In this study, a three-dimensional electrode electrochemical oxidation system was constructed with powdered activated carbon as the particle electrode, graphite as the anode and stainless steel as the cathode, and the electrochemical oxidation degradation effect of DBP simulated wastewater at high altitude was studied. When applying the system to the simulated wastewater, the maximum chemical oxygen demand (COD) removal rate reached 61.75% at a plate spacing of 5 cm, electrolyte and particle-electrode dosages of 12 g and 35 g, respectively, and an electrolytic voltage of 20 V. Electrolyte voltage is the most influential factor in the COD removal rate, followed by plate spacing, electrolyte dosage, and particle electrode dosage. The graphite electrode was confirmed to be higher-value than ruthenium–iridium, titanium mesh, and lead dioxide electrodes.

Keywords: refractory organic matter, three-dimensional electrode, electrochemical oxidation, value

1. Introduction

Refractory organic matter is often detected in natural water, municipal sewage, landfill leachate and so on (Dong et al. 2023, Wu et al. 2022). Phthalates (PAEs) are the most abundantly produced and widely used synthetic organic compounds worldwide. One PAE is dibutyl phthalate (DBP), a typical refractory organic matter that can be released into the environment during manufacture and use. Enriched DBP in the environment can spread through the food chain and has a long hydrolysis half-life, seriously threatening the safety of aquatic ecosystems. Accordingly, many countries list DBP as an environmental priority pollutant (Sun et al. 2020). Therefore, DBP was chosen as the research object for this study.

Refractory organic matter is usually treated with physicochemical methods, biochemical methods, or the advanced oxidation method. The main physicochemical methods are adsorption, coagulation, filtration, and neutralisation. These methods concentrate, enrich, and ultimately remove PAEs from water but cannot completely degrade the PAEs. The main biochemical methods are the activated sludge method, MBR, and constructed wetlands, in which microorganisms perform oxidation degradation of water pollutants for growth and reproduction. Such processes are slow and produce a large amount of sludge (Wang et al. 2019); moreover, PAE residues in the environment inhibit the metabolic functions of microorganisms, disturb the microbial ecological balance, and affect the growth of animals and plants (Wang et al. 2021). As Qinghai province is located in the northeastern edge of the Qinghai-Tibet Plateau, the average altitude is more than 3000 m, the provincial capital Xining air pressure is 761 hPa, which is 76% of Beijing, the annual average temperature is 6°C, studies have shown that the average oxygen concentration of Qilian Mountains in summer 20.47%. The average oxygen concentration in the Qilian Mountains is 20.47% in summer and 20.16% in winter (Shi et al. 2021). Advanced oxidation methods mainly include ozone oxidation, the Fenton reaction, electrochemistry, photolysis, sonolysis (Saravanan et al. 2022), photocatalysis (Koe et al. 2020), wet oxidation (García et al. 2020), and supercritical water oxidation (Wei et al. 2021). These processes generate many free radicals with strong oxidation ability for pollutant degradation.

Qinghai Province is rich in power resources. Reportedly, Qinghai Province supplied more than 31% of the clean electricity to the 19th Asian Games in Hangzhou. Therefore, the electrochemical method is the method of choice for treating refractory organic matter in Qinghai. Other advantages of electrochemical oxidation (EO) technology are simple treatment equipment, mild treatment conditions, convenient operation, good controllability, and no secondary pollution. This environmentally friendly technology can be applied to all kinds of wastewater treatment (Qiao et al. 2021) but is especially suitable for organic wastewater that is difficult to degrade or cannot be effectively treated by general chemical oxidation methods (Li et al. 2021). Xu et al. reported a chemical oxygen demand (COD) removal rate of 94.4% during the electrochemical oxidative degradation of wastewater containing levofloxacin (Xu et al. 2023). Wu et al. performed an EO degradation of pharmaceutical wastewater, achieving a removal rate of 100% (Wu et al. 2023).

The three-dimensional electrode system, constructed by filling a particle electrode between the anode and cathode electrodes, lowers the mass-transfer resistance of EO and improves the current efficiency from those of the traditional two-dimensional electrode systems (Deng et al. 2020, Shi et al. 2020). Zhu et al. reported a 2–7 times higher removal rate of p-nitrophenol and COD in a three-dimensional electrode system than in a two-dimensional electrode system (Zhu et al. 2011). Kong et al. treated anionic surfactants with a three-dimensional electrode system, obtaining a COD removal rate of 86% (Kong et al. 2006). Shi et al. degraded amoxicillin (AMX) in an activated carbon three-dimensional electrode system. They reported an AMX removal rate of 98.98% (Shi et al. 2020). Yu et al. treated landfill leachate with three-dimensional electrode EO technology. COD and ammonia nitrogen removal rates reached 72.9% and 99.9%, respectively, and the treated landfill leachate was clear and transparent (Yu et al. 2020).

Most of the current research on EO treatment technology has focused on electrode materials (cathode materials, anode materials, and particle electrodes). Yang et al. prepared particle electrodes from raw materials (flotation tailings, garden soil, and soluble starch) and adopted a ruthenium–iridium plated titanium network as the electrode for the EO treatment of tetracycline wastewater. The tetracycline removal rate reached 59.87% (Yang et al. 2021). Pourzamani et al. used multi-walled carbon nanotubes as the particle electrodes in a three-dimensional electrochemical electro-oxidation treatment of diclofen acid (DCF) in aqueous solution on a Ti/RuO_2–TiO_2 electrode, obtaining a DCF removal rate of 99.61% (Pourzamani et al. 2018). Despite their efficacy, these electrode materials are complex or expensive to fabricate.

Many present studies consider only the removal efficiency, but the investment cost of sewage treatment is also important because the government or investors must analyse the economic cost when assessing the feasibility of the water treatment process (Hernández-Chover et al. 2018, Chen et al. 2024). In actual implementations of the process, costly technology is an obstacle, and recent research on water treatment is leaning toward cheaper materials and new low-cost processing technology (Dong et al. 2022).

This study introduces an electrochemical system for the EO degradation of refractory organic matter (DBP) with inexpensive and easily obtained electrode materials: graphite, stainless steel, and activated carbon. The effectiveness of EO technology in treating refractory organic pollutants on the cold, high-altitude Qinghai–Tibet Plateau is evaluated.

2. Materials and Methods

2.1. Main instruments and chemicals

The main equipment and chemicals were a UV–visible spectrophotometer (TU-1810, Beijing Puyang General Instrument Co., Ltd.), dibutyl phthalate (Analyte Pure, Sinopharm Chemical Reagent Co., Ltd.), anhydrous ethanol (Analyte Pure, Tianjin Fuyu Fine Chemical Co., Ltd.), and sodium sulfate (Analyte pure, Tianjin Zhiyuan Chemical Reagent Co., Ltd.).

2.2. Experimental setup

The EO degradation device comprises an adjustable DC-voltage regulated power supply, an electrolytic cell, an electrode (sized 100 mm × 100 mm × 5 mm with a graphite anode and a stainless steel cathode), a particle electrode (powdered activated carbon (PAC) after saturated adsorption of simulated wastewater), and an electrolyte (sodium sulfate). The electrode spacing (cm), amounts of electrolyte and particle electrode (both in g), and the initial electrolytic voltage V (hereafter referred to as the electrolytic voltage) influence the electrochemical reaction. The simulated wastewater with DBP concentration of 10 mg/L was degraded by electrochemical oxidation.

2.3. Experimental design of the response surface method

The response surface method (RSM) identifies the variable conditions that best predict the target response (maximum degradation efficiency) (Körbahti et al. 2007) and optimises the influential parameters (Fu et al. 2007). The Box–Behnken method is the most efficient RSM method, requiring the smallest number of experiments (Zhang et al. 2010). In the present experiment, the plate spacing, electrolyte dosage, particle electrode dosage, and electrolytic voltage were taken as the independent variables, and the COD removal rate was the dependent variable. The optimal experimental conditions that maximise the degradation rate were obtained through a single-factor experiment (fixing the current at 3.4 A, the plate spacing at 5 cm, the electrolytic voltage at 15 V, and the PAC dosage at 30 g. At a sodium sulfate dose of 12 g, the COD degradation rate reached 50.9% after 120 min of electrolysis). Table 1 gives the level codes of the design factors.

Table 1. Experimental design

Independent variables	Code levels		
	-1	0	+1
A: plate spacing /cm	4	5	6
B: electrolyte dosage /g	9	12	15
C: particle electrode dosage /g	25	30	35
D: electrolytic voltage /V	10	15	20

The variable correlations were described using a second-order polynomial as follows (Pourzamani et al. 2018), to optimise the COD removal rate:

$$Y = \beta_0 + \sum_{i=1}^{n} \beta_i X_i + \sum_{i=1}^{n} \beta_{ii} X_i^2 + \sum_{i=1}^{n-1} \sum_{i=1}^{n} \beta_{ij} X_i X_j \quad (1)$$

where:
Y – the dependent variable (COD removal rate),
β_0 – constant,
β_i, β_{ii}, and β_{ij} – the linear, second-order, and interaction coefficients, respectively,
X_i and X_j – the parameter coding values,
n – the number of parameters.

2.4. Analytical method

2.4.1. COD removal rate

The rapid digestion method determines the DBP degradation effect, expressed as the removal rate of COD. The COD removal rate is calculated as (2) (Li H. et al. 2021):

$$COD \text{ removal rate } (\%) = \frac{C_0 - C_t}{C_0} \times 100\% \quad (2)$$

where:
C_0 – the initial COD level of the reaction (mg/L),
C_t – the COD level at time t during the reaction (mg/L).

2.4.2. Value Engineering

Value engineering is a modern management method that minimises the cost of acquiring the necessary basic skills (Youssef et al. 2023). Value engineering attempts to improve a project's value, function, and performance while reducing the cost as much as possible (Ibusuki et al. 2007). The same or a similar processing effect can be achieved by replacing expensive materials with low-cost materials to maximise the value. The value engineering formula is (Li X. et al. 2021):

$$VE = F/C \quad (3)$$

where:
VE – the value,
F – the function, in the present study, F is the COD removal rate,
C – the cost; in the present study, C is the purchase price of electrode material per unit area multiplied by unit energy consumption.

The unit energy consumption is calculated as (4) (Zou et al. 2017).

$$E = \frac{1000 \cdot U \cdot I \cdot t}{V \cdot \Delta COD} \quad (4)$$

where:
E – the unit energy consumption,
U – the electrolytic voltage,
I – the electrolytic current,
t – the eaction time,
V – the volume of wastewater,
△COD – the COD removed within t time.

3. Results and Discussion

3.1. Optimisation of the COD removal rate using the RSM method

The design matrix and experimental results are given in Table 2.

Table 2. Design matrix in coded units and the experimental responses

Run	Plate spacing/cm	Electrolyte dosage/g	Particle electrode dosage/g	Electrolytic voltage/V	COD removal rate/%	
					Actual value	Predicted value
1	1	-1	0	0	33.4	36.32
2	0	1	0	-1	34.07	35.27
3	1	0	0	1	59.84	58.97
4	0	-1	0	1	61.32	58.31
5	-1	0	0	-1	39.69	39.78
6	0	-1	-1	0	45.92	45.45
7	0	1	1	0	52.14	51.84
8	0	0	0	0	59.84	58.36
9	0	0	0	0	57.76	58.36
10	0	-1	1	0	49.47	49.44
11	0	0	0	0	58.97	58.36
12	0	0	1	-1	36.14	38.42
13	-1	-1	0	0	54.21	55.06
14	0	1	-1	0	50.66	49.91
15	1	1	0	0	49.47	51.21
16	0	-1	0	-1	32.88	29.62
17	1	0	1	0	54.80	52.33
18	0	1	0	1	58.06	59.51
19	0	0	-1	1	61.62	61.92
20	0	0	0	0	59.45	58.36
21	-1	0	1	0	52.73	52.79
22	-1	1	0	0	50.36	47.02
23	0	0	-1	-1	31.7	33.83
24	1	0	0	-1	31.4	28.95
25	-1	0	0	1	61.02	62.69
26	1	0	-1	0	44.43	42.56
27	0	0	0	0	57.38	58.36
28	0	0	1	1	62.80	63.25
29	-1	0	-1	0	55.99	56.65

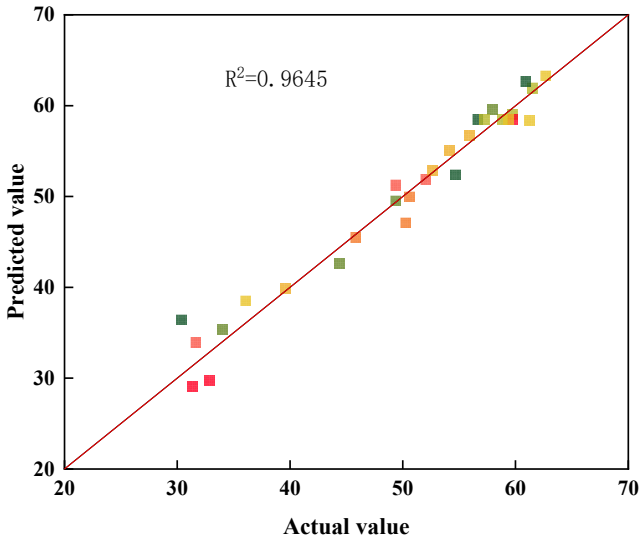

Fig. 1. Predicted versus experimentally determined COD removal rates

Based on the RSM results, the variable–response relationships were analysed through a multi-regression analysis. Eqs (5) and (6) give the regression equations of the actual and coding factors, respectively:

$$Y = -152.39 - 6.56A + 10.50B + 4.56C + 10.30D + 1.91AB + 0.68AC + 0.36AD - 0.03BC - 0.07BD - 0.03CD - 4.58A^2 - 0.72B^2 - 0.11C^2 - 0.25D^2 \quad (5)$$

$$Y = 58.48 - 3.64A + 1.71B + 1.48C + 13.23D + 5.73AB + 3.41AC + 1.78AD - 0.52BC - 1.11BD - 0.82CD - 4.58A^2 - 6.50B^2 - 2.82C^2 - 6.30D^2 \quad (6)$$

where:
Y – the COD removal rate (%),
A – the plate spacing (cm),
B and C – the electrolyte and particle electrode dosages, respectively (g),
D – the electrolytic voltage (V).

Table 2 and Figure 1 show that the predicted COD removal rate closely approximates the experimental value. As can be seen from Table 3, the determination coefficient R^2 of the regression equation is 0.9645 (>0.80), which indicates that the model is well-fitted and the predicted experimental data is relatively accurate. The correlation coefficient of prediction R^2_{pre} and the adjustment coefficient R^2_{adj} are reasonably consistent (difference = 0.12 < 0.2), indicating that the model well reflects the relationship between the independent variables and response value. The coefficient of variation is acceptable (CV = 5.61%) (Pourzamani et al. 2018), and the precision (16.9480) far exceeds 4.0, indicating the experiment has high reliability and accuracy.

Table 3. Statistical analysis of errors in the regression equation

Item	Std.Dev.	Mean	C.V. %	R^2	R^2_{adj}	R^2_{pre}	Adeq Precision
Value	2.81	50.12	5.61	0.9645	0.9290	0.8053	16.9480

Equations (5) and (6) show that plate spacing negatively influences the COD removal rate while the other factors exert a positive effect.

3.2. Analysis of variance

Analysis of Variance is a statistical technique that tests the importance of the factors influencing the model (Pourzamani et al. 2018). As shown in Table 4, the fitting of the binomial model is extremely significant, the missing fitting term is not significant, and the F-value of the model is 27.18, indicating that the model has high significance. The influences of the four independent variables on the COD removal rate declined in the following order: electrolytic voltage D > plate spacing A > electrolyte dosage B > particle electrode dosage C.

Table 4. Analysis of variance of the regression equation

Source	Sum of Squares	df	Mean Squares	F-value	p-value	
Model	3013.43	14	215.24	27.18	< 0.0001	significant
A: plate spacing	158.85	1	158.85	20.06	0.0005	
B: electrolyte dosage	35.23	1	35.23	4.45	0.0534	
C: particle electrode dosage	26.28	1	26.28	3.32	0.0899	
D: electrolytic voltage	2100.92	1	2100.92	265.28	< 0.0001	
AB	131.33	1	131.33	16.58	0.0011	
AC	46.44	1	46.44	5.86	0.0296	
AD	12.64	1	12.64	1.60	0.2271	
BC	1.07	1	1.07	0.1353	0.7185	
BD	4.95	1	4.95	0.6251	0.4423	
CD	2.66	1	2.66	0.3355	0.5716	
A^2	135.91	1	135.91	17.16	0.0010	
B^2	274.05	1	274.05	34.60	< 0.0001	
C^2	51.58	1	51.58	6.51	0.0230	
D^2	257.65	1	257.65	32.53	< 0.0001	
Residual	110.87	14	7.92	–	–	
Lack of fit	103.67	10	10.37	5.76	0.0531	not significant
Pure error	7.20	4	1.80	–	–	
Cor. total	3124.30	28	–	–	–	

Note: $P > 0.05$ means insignificant; $P \leq 0.05$ means significant; $P < 0.0001$ means extremely significant.

3.3. Interaction effects of various factors on the degradation rate

Figure 2 compares the results of the four independent variables. At the centre point A = 5 cm, B = 12 g, C = 30 g, and D = 15 V, the steeper curve of D than of the other variables indicates that COD removal rate increases significantly with increasing electrolytic voltage. The second steepest is curve A, indicating a significant decrease in COD removal rate with increasing plate spacing. The B and C curves change insignificantly, indicating that changing the electrolyte and particle electrode dosages little affects the COD degradation.

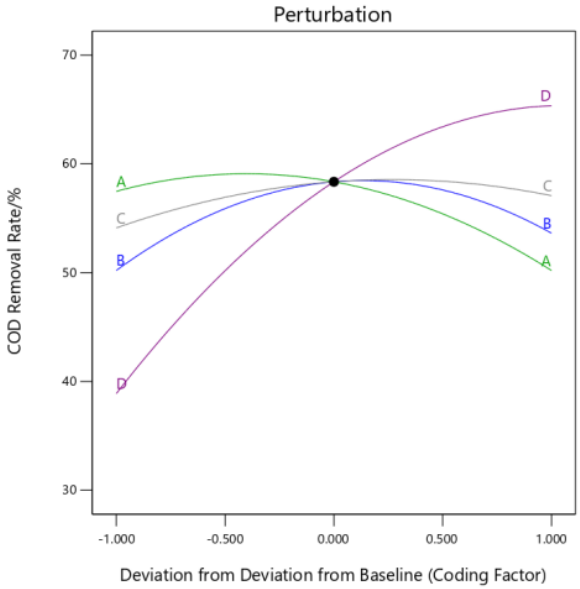

Fig. 2. Disturbance curves of the response variables (A: plate spacing, cm; B: electrolyte dosage, g; C: particle electrode dosage, g; D: electrolytic voltage, V)

To evaluate the interaction effects of the independent variables, the influences of the experimental conditions on the COD removal rate were visualised by plotting the response surfaces and contours based on the RSM equation (Eq. 5). The results are shown in Figure 3.

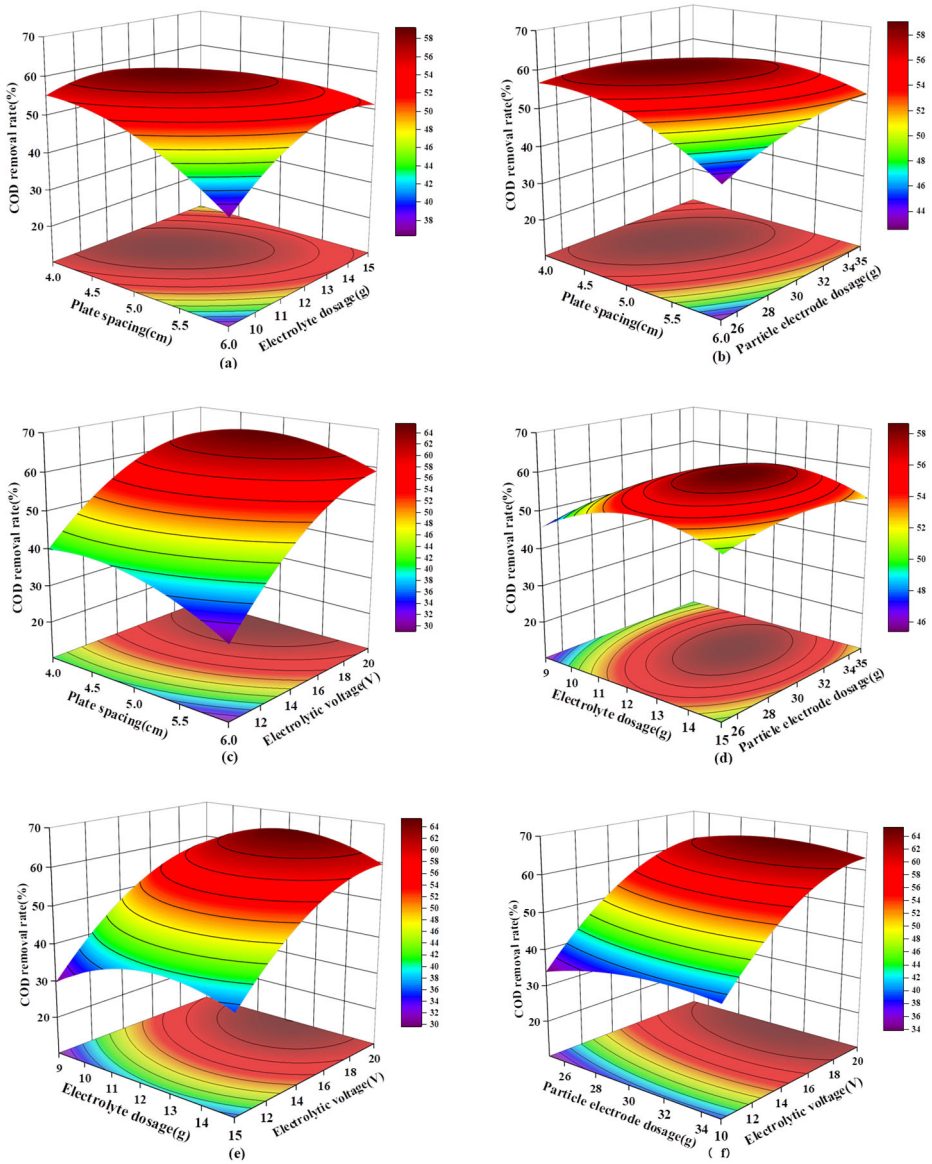

Fig. 3. RSM plots of COD removal rate (Interaction effects of plate spacing and (a) electrolyte dosage with C = 30 g, D = 15 V, (b) particle electrode dosage with B = 12 g, D = 15 V, (c) electrolytic voltage with B = 12 g, C = 30 g; interaction effects of electrolyte dosage, (d) particle electrode dosage with A = 5 cm, D = 15 V, (e) electrolytic voltage with A = 5 cm, C = 30 g, (f) electrolytic voltage with A = 5 cm, B = 12 g)

In the contour diagrams of Figure 3, the electrolyte dosage shows no obvious interaction with particle electrode dosage but does interact with the other influencing factors. The COD removal rate is more strongly influenced by plate spacing than by electrolyte dosage and particle electrode dosage (Figure 3 (a), (b)) and more strongly influenced by the electrolytic voltage than by plate spacing, electrolyte dosage, and particle electrode dosage (Figure 3 (c)-(f)).

The corresponding surface diagrams in Figure 3 (c), (e) and (f) show that increasing the voltage increases the removal rate of COD (Darvishmotevalli et al. 2019, Hu et al. 2024) by up to 62.8%. This occurs because increasing the electrolyte concentration and voltage increase simultaneously the conductivity and current, thus accelerating the reaction speed of electrochemical damage (Körbahti et al. 2007). Further increasing the voltage decreases the COD removal rate, mainly because a high electrolytic voltage aggravates the occurrence of side reactions and produces many bubbles that inhibit the mass transfer (Li et al. 2021). As shown in Eqs. (7) and (8).

$$H_2O - e^- \rightarrow O_2 + H^+ \quad (7)$$

$$H_2O + e^- \rightarrow H_2 + OH^- \quad (8)$$

The curved surface diagrams in Figure 3 (a), (b) and (c) reveal a gradual decrease in COD removal rate with increasing plate spacing. This trend is explained by the increasing dominance of indirect oxidation with increasing plate spacing, whereas direct oxidation of electrodes is the main action of COD removal (Zhang et al. 2011). As shown in Eqs. (9) and (10).

$$R \rightarrow R + e^- \tag{9}$$

$$H_2O \rightarrow \cdot OH + H^+ + e^- \tag{10}$$

The curved surface diagrams in Figure 3 (b), (d), and (f) confirm a gradual rise in COD removal rate with increasing particle electrode dosage, which is mainly explained by the corresponding increases in particle electrode, effective electrode area, and number of catalytic active sites of the electro-oxidation reaction. Accordingly, the mass transfer distance is greatly reduced and the electrical conductivity increases, boosting the organic matter degradation efficiency (Ma et al. 2021). However, an excessive dosage decreases the COD removal rate, partly because the number of effectively suspended polarised particles saturates, and the outermost layer of the electrochemical reaction electrode tends to stabilise. The decrease in COD removal is also contributed to by an excessive short-circuit current at high particle electrode dosages (Li et al. 2021).

3.4. Parameter optimisation and verification

The optimal parameter values, determined using Design-Expert 13, are 5 cm for the inter-plate distance, 12 g and 35 g for the added electrolyte and particle electrode, respectively, and 20 V for the electrolytic voltage. The optimal COD removal rate is 63.25%. Table 5 gives the results of electrochemical degradation experiments conducted under the above experimental conditions.

Table 5. Parallel verification experiment

Exp. No.	COD removal rate/%	Mean value/%	Relative error/%
1	61.90	61.75	2.37
2	62.50		
3	60.85		

In the verification experiment, the error between the measured and predicted values was only 2.37% (<5%), indicating the high reliability of the model.

3.5. Value analysis

Adopting the response-surface optimised parameters, EO experiments were carried out using electrodes of different materials: ruthenium–iridium stainless steel, titanium mesh stainless steel, and lead dioxide stainless steel. The experimental results are shown in Table 6.

Table 6. Value analysis of DBP degradation

Anode	Cathode	Cost	COD removal rate	Unit energy consumption	VE
Ruthenium-iridium	Stainless steel	2	66.7	29.76	0.0112
Titanium mesh		1	66.2	28.12	0.0235
Lead dioxide		1.5	65.9	27.43	0.0160
Graphite		0.5	61.8	29.19	0.0424

As shown in Table 6, under the same experimental conditions, the ruthenium-iridium, titanium mesh and lead dioxide have higher COD removal efficiency, and graphite has the lowest. Still, the value of the graphite electrode is the highest.

4. Conclusions

The main findings are summarised below.

1. The effects of the four independent variables on the COD removal rate decrease in the order of electrolytic voltage >plate spacing >electrolyte dosage >particle electrode dosage.
2. With the increase of electrolytic voltage, the removal rate of COD increases significantly. With the increase of plate spacing, the removal rate of COD decreases significantly. The change in electrolyte and particle electrode dosage has no significant effect on COD degradation.

3. Through a parameter optimisation analysis, the COD removal rate was maximised (at 63.25%) at a pad spacing of 5 cm, an electrolyte dosage of 12 g, a particle electrode dosage of 35 g, and an electrolytic voltage of 20 V. Experimental verification identified an error of only 2.37% (<5%) between the measured and predicted values.
4. The value of the graphite electrode is the highest.

Declaration of competing interest

The authors declare that they have no known competing financial interests or personal relationships that could have appeared to influence the work reported in this paper.

Acknowledgement

The authors extend their appreciation to the Qinghai University Youth Research Fund Project for funding this work, and grant number is 2021-QGY-12. The authors duly acknowledged the Qinghai University, China, for the technical support.

References

Chen, F., Jiang, F., Zhu, Y., Hua, Z., Wang, L., Ma, J., ... Tsiakaras, P. (2024). Three-dimensional electro-Fenton system with steel-slag based particle electrode for the treatment of refinery spent caustic. *Journal of Environmental Chemical Engineering*, *12*(2), 112429.

Darvishmotevalli, M., Zarei, A., Moradnia, M., Noorisepehr, M., Mohammadi, H. (2019). Optimisation of saline wastewater treatment using electrochemical oxidation process: prediction by RSM method. *MethodsX*, *6*, 1101-1113.

Deng, D., Wu, X., Li, M., Qian, S., Tang, B., Wei, S., Zhang, J. (2020). Electrochemical degradation of three phthalate esters in synthetic wastewater by using a Ce-doped Ti/PbO_2 electrode. *Chemosphere*, *259*, 127488.

Dong, S., Gong, Y., Zeng, Z., Chen, S., Ye, J., Wang, Z., Dionysiou, D. D. (2023). Dissolved organic matter promotes photocatalytic degradation of refractory organic pollutants in water by forming hydrogen bonding with photocatalyst. *Water Research*, *242*, 120297.

Dong, Y., Wu, H., Yang, F., Gray, S. (2022). Cost and efficiency perspectives of ceramic membranes for water treatment. *Water Research*, *220*, 118629.

Fu, J., Zhao, Y., Wu, Q. (2007). Optimising photoelectrocatalytic oxidation of fulvic acid using response surface methodology. *Journal of Hazardous Materials*, *144*(1-2), 499-505.

García, M., Collado, S., Oulego, P., Díaz, M. (2020). The wet oxidation of aqueous humic acids. *Journal of hazardous materials*, *396*, 122402.

Hernández-Chover, V., Bellver-Domingo, Á., Hernández-Sancho, F. (2018). Efficiency of wastewater treatment facilities: The influence of scale economies. *Journal of environmental management*, *228*, 77-84.

Hu, X., Huang, L., Sun, T., Gao, Z., Qu, Z. (2024). TiO_2-loading modification on graphene aerogel particle electrode for electrochemical oxidation of TCH wastewater with low electrolyte concentration: Performance and mechanism. *Journal of Electroanalytical Chemistry*, *962*, 118268.

Ibusuki, U., Kaminski, P. C. (2007). Product development process with focus on value engineering and target-costing: A case study in an automotive company. *International Journal of production economics*, *105*(2), 459-474.

Koe, W. S., Lee, J. W., Chong, W. C., Pang, Y. L., Sim, L. C. (2020). An overview of photocatalytic degradation: photocatalysts, mechanisms, and development of photocatalytic membrane. *Environmental Science and Pollution Research*, *27*(3), 2522-2565.

Kong, W., Wang, B., Ma, H., Gu, L. (2006). Electrochemical treatment of anionic surfactants in synthetic wastewater with three-dimensional electrodes. *Journal of hazardous materials*, *137*(3), 1532-1537.

Körbahti, B.K. (2007). Response surface optimisation of electrochemical treatment of textile dye wastewater. *Journal of hazardous materials*, *145*(1-2), 277-286.

Körbahti, B.K., Aktaş, N., Tanyolaç, A. (2007). Optimisation of electrochemical treatment of industrial paint wastewater with response surface methodology. *Journal of Hazardous Materials*, *148*(1-2), 83-90.

Li, H., Yang, H., Cheng, J., Hu, C., Yang, Z., Wu, C. (2021). Three-dimensional particle electrode system treatment of organic wastewater: A general review based on patents. *Journal of Cleaner Production*, *308*, 127324.

Li, X., Wang, C., Alashwal, A. (2021). Case study on BIM and value engineering integration for construction cost control. *Advances in Civil Engineering*, *2021*(1), 8849303.

Ma, J., Gao, M., Shi, H., Ni, J., Xu, Y., Wang, Q. (2021). Progress in research and development of particle electrodes for three-dimensional electrochemical treatment of wastewater: A review. *Environmental Science and Pollution Research*, *28*, 47800-47824.

Pourzamani, H., Mengelizadeh, N., Hajizadeh, Y., Mohammadi, H. (2018). Electrochemical degradation of diclofenac using three-dimensional electrode reactor with multi-walled carbon nanotubes. *Environmental Science and Pollution Research*, *25*, 24746-24763.

Qiao, J., Xiong, Y. (2021). Electrochemical oxidation technology: A review of its application in high-efficiency treatment of wastewater containing persistent organic pollutants. *Journal of Water Process Engineering*, *44*, 102308.

Saravanan, A., Deivayanai, V. C., Kumar, P. S., Rangasamy, G., Hemavathy, R. V., Harshana, T., ... Alagumalai, K. (2022). A detailed review on advanced oxidation process in treatment of wastewater: Mechanism, challenges and future outlook. *Chemosphere*, *308*, 136524.

Shi, H., Wang, Q., Ni, J., Xu, Y., Song, N., Gao, M. (2020). Highly efficient removal of amoxicillin from water by three-dimensional electrode system within granular activated carbon as particle electrode. *Journal of Water Process Engineering*, *38*, 101656.

Shi, P., Chen, Y., Zhang, G., Tang, H., Chen, Z., Yu, D., ... Gong, P. (2021). Factors contributing to spatial–temporal variations of observed oxygen concentration over the Qinghai-Tibetan Plateau. *Scientific reports*, *11*(1), 17338.

Sun, J., Wei, B., Mei, Q., An, Z., Wang, X., Han, D., ... He, M. (2020). Theoretical investigation on the degradation of dibutyl phthalate initiated by OH and SO_4·– in aqueous solution: Mechanism, kinetics and ecotoxicity assessment. *Chemical Engineering Journal*, *382*, 122791.

Wang, G., Zhang, Q., Chen, Q., Ma, X., Xin, Y., Zhu, X., ... Xiao, Z. (2019). Photocatalytic degradation performance and mechanism of dibutyl phthalate by graphene/TiO_2 nanotube array photoelectrodes. *Chemical Engineering Journal*, *358*, 1083-1090.

Wang, X., Wu, H., Wang, X., Wang, H., Zhao, K., Ma, B., Lu, Z. (2021). Network-directed isolation of the cooperator Pseudomonas aeruginosa ZM03 enhanced the dibutyl phthalate degradation capacity of Arthrobacter nicotianae ZM05 under pH stress. *Journal of Hazardous Materials*, *410*, 124667.

Wei, N., Xu, D., Hao, B., Guo, S., Guo, Y., Wang, S. (2021). Chemical reactions of organic compounds in supercritical water gasification and oxidation. *Water Research*, *190*, 116634.

Wu, C., Ge, J., Gu, F., Bai, L. (2023). Electrochemical oxidation technique to pharmaceutical pollutants removal. *Chemosphere*, *337*, 139373.

Wu, R., Li, Y. Y., Liu, J. (2022). Refractory dissolved organic matter as carbon source for advanced nitrogen removal from mature landfill leachate: A review and prospective application. *Journal of Cleaner Production*, *380*, 134962.

Xu, T., Tang, X., Qiu, M., Lv, X., Shi, Y., Zhou, Y., ... Ge, S. (2023). Degradation of levofloxacin from antibiotic wastewater by pulse electrochemical oxidation with BDD electrode. *Journal of environmental management*, *344*, 118718.

Yang, S., Feng, Y., Gao, D., Wang, X., Suo, N., Yu, Y., Zhang, S. (2021). Electrocatalysis degradation of tetracycline in a three-dimensional aeration electrocatalysis reactor (3D-AER) with a flotation-tailings particle electrode (FPE): Physicochemical properties, influencing factors and the degradation mechanism. *Journal of Hazardous Materials*, *407*, 124361.

Youssef, M., AlDeep, S. M. H., Olwan, M. M. (2023). Value engineering: Case study of Libyan educational buildings. *Alexandria Engineering Journal*, *76*, 735-746.

Yu, D., Cui, J., Li, X., Zhang, H., Pei, Y. (2020). Electrochemical treatment of organic pollutants in landfill leachate using a three-dimensional electrode system. *Chemosphere*, *243*, 125438.

Zhang, H., Li, Y., Wu, X., Zhang, Y., Zhang, D. (2010). Application of response surface methodology to the treatment landfill leachate in a three-dimensional electrochemical reactor. *Waste Management*, *30*(11), 2096-2102.

Zhang, H., Ran, X., Wu, X., Zhang, D. (2011). Evaluation of electro-oxidation of biologically treated landfill leachate using response surface methodology. *Journal of hazardous materials*, *188*(1-3), 261-268.

Zhu, X., Ni, J., Xing, X., Li, H., Jiang, Y. (2011). Synergies between electrochemical oxidation and activated carbon adsorption in three-dimensional boron-doped diamond anode system. *Electrochimica Acta*, *56*(3), 1270-1274.

Zou, J., Peng, X., Li, M., Xiong, Y., Wang, B., Dong, F., Wang, B. (2017). Electrochemical oxidation of COD from real textile wastewaters: kinetic study and energy consumption. *Chemosphere*, *171*, 332-338.